THE UNIVERSITY OF MICHIGAN

College of Engineering

Department of Mechanical Engineering

Cavitation and Multiphase Flow Laboratory

Report No. UMICH 03371-16-T

LIQUID DROPLET IMPINGEMENT STUDIES AT UNIVERSITY OF MICHIGAN

by

F. G. Hammitt*
Y. C. Huang**

(Heat and Fluid Flow in Steam and Gas Turbine Plant Symposium)
(University of Warwick, April 1973)

Financial Support Provided by:

National Science Foundation
Grant No. GK-730

May 1972

*Professor-in-Charge, Cavitation and Multiphase Flow Laboratory, Mech. Engr. Dept., University of Michigan, Ann Arbor, Michigan

**Engineer, Gibbs and Hill, N. Y., N. Y., (formerly doctoral candidate, Mech. Engr. Dept., University of Michigan, Ann Arbor, Michigan)

LIST OF FIGURES

TABLES

F. G. Hammitt, PhD and Y. C. Huang, PhD
Cavitation and Multiphase Flow Laboratory, Dept. of Mech Engr., University of Michigan, Ann Arbor, Michigan
(Y. C. Huang presently with Gibbs and Hill, N. Y., N. Y.)

Liquid Droplet Impingement Studies at University of Michigan

SYNOPSIS Work at the University of Michigan relating to the turbine droplet impingement program is described. While this includes the development of a low-pressure wet-steam tunnel for studies of droplet formation and also experiments upon material resistance and droplet impingement, it primarily concerns numerical studies of droplet impingement upon target surfaces. Results include pressures and velocities within the drop and upon target surfaces. Pressures are compared with a "slab" collision model ("corrected water hammer pressure") and with "simple water hammer", not involving correction for actual shock wave velocity in the compressed liquid. Maximum pressures for three-dimensional drops are well less than the "slab" model, but are essentially independent of impact velocity if normalized to this pressure. They exceed "simple water hammer pressure" only for velocities of the order of 750 m/s and larger.

INTRODUCTION

1. Liquid droplet impingement erosion is a serious and limiting phenomenon today in various important technological fields such as large steam (or other vapor) turbines, high-speed fixed-wing aircraft and helicopter rotors, to name three of the most prominent. Also, cavitation applications, such as high-speed ships, should be included because of the well-recognized similarities between these different forms of erosive attack.

2. In all cases the overall problem involves several phases, e.g.,
a) Dynamics of liquid phase (and droplets) during their nucleation and traverse to the eroded region. Droplet size and shape, and impact velocity and angle, are thus determined.
b) Interaction between droplet and eroded material during single impact.
c) Material failure after one of more impacts, thus creating erosion.
Our laboratory is actively researching all of these three phases. However, of the three, we have in the past concerned ourselves primarily with b), interaction between droplet and material during single impact, and c) material failure after one or more impacts. The present paper will discuss the results, so far obtained and in progress, particularly the analytical work which has been done under subject b).

3. Our total program has included experimental studies of material resistance and impact using a "water gun" device capable of projecting liquid droplets (i.e., elongated slugs) at velocities up to 600 m/s and at repetition rates of ~30/min., as well as numerous cavitation damage studies. These are covered elsewhere (1-5). In addition, we have recently commenced the development of a low pressure steam tunnel for the study of wet steam flows, particularly related to problems of moisture film build-up and droplet separation.

4. The present paper discussed numerical studies of pressures, velocities, stresses, and deformations occurring during droplet impact. This work has been primarily based on the doctoral dissertation of one of the authors (6, 7). It has included water Mach numbers up to 0.5 (~750 m/s), spherical and cylindrical droplets, as well as a combined shape which is perhaps more realistic of real impacts. For given fluid physical parameters and for a completely rigid surface (which was assumed in our initial study) we have shown that only the parameters of liquid Mach number and droplet shape are important. Our study is continuing to include the effects of surface deformation (8) and finite material elasticity. These latter are particularly important for elastomeric coating materials, not normally involved for steam turbine blading, but important in numerous other applications.

5. The paper will present a summary of the results from this continuing study obtained up to the time of writing.

TURBINE-RELATED DROPLET IMPACT WORK AT UNIVERSITY OF MICHIGAN

A. Numerical Studies of Droplet Impact

1. Solution Method

6. Since our work has been predominently concerned with numerical studies of impact, these will be described and summarized first. To our knowledge, this work represents the first relatively comprehensive treatment of the impact problem in the velocity range pertinent to the steam turbine problem and also to aircraft raindrop erosion, i.e., perhaps 200 to 800 m/s. In this velocity range it is not possible to neglect either fluid compressibility

(as might be possible in a very low velocity case) or target material strength (as is sometimes done for hypersonic impact analyses). As is shown by our analysis, for a fully rigid flat surface and for given liquid properties, the only important parameters of the collision in the droplet size (perhaps 1-3mm dia.) and velocity range considered are liquid impact Mach number, droplet shape, and impact angle. Hence the investigation has included the liquid Mach numbers of 0.2 and 0.5 ($\sim$300 and $\sim$750 m/s for cold water). Three droplet shapes have been included, i.e., spherical, cylindrical, and a composite spherical-cylindrical droplet (cylindrical droplet with rounded corners), which it is felt may be the most realistic of the three shapes for most impact cases.

7. The analysis is described in detail elsewhere (6, 7), but for convenience a brief summary will be made here. For most of the numerical studies so far made, a completely rigid flat target surface was assumed. While compressibility of the liquid must be included to obtain realistic results in the velocity range of interest, surface tension and viscosity can be safely ignored compared to pressure and inertia effects for the droplet size range of interest. Under these conditions the equations of continuity and momentum for the liquid drop become;

$$\frac{\partial \rho}{\partial t} + \frac{\partial (\rho u^2)}{\partial z} + \frac{1}{r}\frac{\partial (r\rho v)}{\partial r} = 0 \qquad (1)$$

$$\frac{\partial (\rho u)}{\partial t} + \frac{\partial (\rho u^2)}{\partial z} + \frac{1}{r}\frac{\partial (r\rho vu)}{\partial r} = -\frac{\partial o}{\partial z} \qquad (2)$$

$$\frac{\partial (\rho v)}{\partial t} + \frac{\partial (\rho vu)}{\partial z} + \frac{1}{r}\frac{\partial (r\rho v^2)}{\partial r} = -\frac{\partial}{\partial r} \qquad (3)$$

and a suitable equation of state for water is that of Tait (9):

$$\frac{p + B}{p_o + B} = \left(\frac{\rho}{\rho_o}\right)^A \qquad (4)$$

Values of the constants B and A were chosen to be appropriate for 20°C water, i.e., B = 3047 bars and A = 7.15.

8. Marker particles are imbedded in the deforming liquid boundary to give its location at all times. The marker particles follow the equation of motion for a free body as described by kinematic relations in a Lagrangian formulation (6, 7). The equations are then normalized by the characteristic parameters of the problem to give the following equation set.

$$\frac{\partial p}{\partial t} + A_1\frac{\partial (\rho u)}{\partial z} + A_2\frac{1}{r}\frac{\partial (r\rho v)}{\partial r} = 0 \qquad (5)$$

$$\frac{\partial (\rho u)}{\partial t} + A_1\frac{\partial (\rho u^2)}{\partial z} + A_2\frac{1}{r}\frac{\partial (r\rho vu)}{\partial r} = -B_1\frac{\partial p}{\partial z} \qquad (6)$$

$$\frac{\partial (\rho v)}{\partial t} + A_1\frac{\partial (\rho uv)}{\partial z} + A_2\frac{1}{r}\frac{\partial (r\rho v^2)}{\partial r} = -B_2\frac{\partial p}{\partial r} \qquad (7)$$

$$\frac{p + B}{p_o + B} = \left(\frac{\rho}{\rho_o}\right)^A \qquad (8)$$

$$\frac{d(\rho U)}{dt} = -B_1\frac{dp}{dz} \qquad (9)$$

$$C/C_o = 1 + 2V_o/C_o - 0.1(V_o/C_o)^2 \qquad (10)$$

$$\frac{d(\rho V)}{dt} = -B_2\frac{dp}{dz} \qquad (11)$$

$$Z_m = A_1\int U\,dt \qquad (12)$$

$$R_m = A_2\int V\,dt \qquad (13)$$

9. Characteristic density ρ_c is that of the undisturbed liquid at 1 atm. and 20°C. Characteristic velocity is the impact velocity V_o. Characteristic pressure is the "simple" water hammer pressure (i.e., $\rho_o C_o V_o$). z_o and r_o are the mathematical cell dimensions in the axial and radial directions, respectively. For convenience, these are chosen to be equal. Characteristic time t_c is z_o/C, where C is the (corrected) shock wave velocity defined by Eq. (10) below. We developed this semi-empirical second-power relation to give shock wave velocities corrected for local density change for the purpose of this analysis (10), providing improved accuracy over relations already available (11, e.g.).

10. The initial conditions over the domain of calculation are $p = p_o$ $u = u_o$ and $v = v_o$. u_o and v_o are the initial impact velocities in the axial and radial directions respectively, so that $v_o = 0$ and $u_o = V_o$ for perpendicular impact, the only case which we have so far studied. The appropriate boundary conditions are then:

i) along the axis of symmetry (z), r = 0 and symmetry requires

$$v = 0, \quad \frac{\partial u}{\partial r} = 0, \quad \frac{\partial p}{\partial r} = 0$$

ii) along the impacted rigid surfaces, z = 0, $\frac{\partial v}{\partial z} = 0$ $u = 0$, $\frac{\partial p}{\partial z} = 0$, for the full-slip wall condition here used. We have reported already[12] similar results for a non-slip wall boundary condition.

iii) along the free surface, the first order terms of the continuity equation yields

$$p = p_o, \quad \frac{\partial u_n}{\partial x_n} = \frac{\partial v_t}{\partial x_t} = 0$$

where u_n and v_t are the moving velocity components of the liquid-air interface in the normal x_n and tangential x_t directions of the surface respectively.

iv) along the sides of the finite computational domain, permeable boundary conditions are imposed, in such a way that the normal space derivative of the variable vanishes at the boundary,

$$\frac{\partial u}{\partial z} = 0, \quad \frac{\partial v}{\partial z} = 0, \quad \frac{\partial p}{\partial z} = 0 \text{ at } z = H_1$$

$$\frac{\partial u}{\partial r} = 0, \quad \frac{\partial v}{\partial r} = 0, \quad \frac{\partial p}{\partial r} = 0 \text{ at } r = H_2$$

where H_1 and H_2 are sizes of computational domain in the z- and r- direction respectively.

11. All the above equations are then approximated by finite difference expressions. The problem is solved by advancing the configuration through a set of finite time steps, or computational cycles. Each numerical computational cycle consists of the following steps.

1) Marker particles on the fluid boundary are moved to appropriate new positions.

2) The continuity and momentum equations are used to advance the densities and velocities through the time change of one cycle by an explicit technique.

3) The pressures are calculated as a function of densities according to the equation of state, assuming a quasi-steady process for each time increment.

4) Boundary condition values and time counters are adjusted to prepare the next computational cycle.

12. Our numerical scheme (ComCAM)* was developed from a combination of the Particle-in-Cell (PIC) method (13), the Marker-and-Cell (MAC) method (14), and the Lax-Wendroff two-step nine-point Eulerian scheme (15). It overcomes some of the difficulties of each, while maintaining most of the advantages at least for the present problem, such as the compressibility of a continuous fluid and the history of a free surface.

13. The program was first used to solve the two-dimensional axisymmetrical droplet impact problem, which is that leading to the classical one-dimensional water-hammer result when a rigid-tube non-permeable shell boundary is imposed. Good agreement with the exact solution for this idealized problem was found (6, 7) and numerical oscillations with our ConCAM method were found to be suitably small.

2. Numerical Results of ConCAM

a. General scope of results

14. The numerical results of the studies so far performed are very numerous and cannot be fully reported here. Full details are available elsewhere (6, 7, 8, 10, e.g.). However, the general scope of the results can be given, and some of those which are considered of primary importance.

15. In general, all but one preliminary numerical study (8) have utilized a fully-rigid flat target surface, upon which both full-slip and non-slip boundary conditions were studied. Ref. 8 involves a non-rigid surface, such as very soft elastomeric coating, for which material reaction exists only in terms of inertia. However, only tentative preliminary results have been obtained to the time of this paper.

16. Only perpendicular impacts have so far been studied, and these have been limited to the impact Mach numbers (referred to the sonic velocity of the undisturbed liquid) of 0.2 and 0.5 (300 and 750 m/s). Cylindrical, spherical, and a composite cylindrical-spherical droplet shape have been investigated. Their initial profiles and later pressure contours are shown in Fig. 1, 2. 3. The composite shape is believed most typical of actual impacting drops such as encountered in the turbine application.

17. The independent variables of the problem are normalized axial and radial coordinates and time. In terms of these, for the other restricting conditions discussed above, the problem is fully described in terms of geometry (droplet shape and impact angle) and impact liquid Mach number. Hence, the results are general in terms of scale. To assist physical interpretation of the results, the units of the non-dimensional time are microseconds if droplet diameter is 2 mm, a typical diameter for damaging droplets in turbine flows or aircraft rain erosion. For such collisions, pressures exerted upon the target surface are of the order of the water hammer pressure (rather than of the normal stagnation pressure) only during the initial small fraction of a microsecond. They approach quite closely the ordinary stagnation pressure after 2-3 μs.

18. Computed quantities include pressure and velocity throughout the impacting droplet (including the interface with target surface), as well as the coordinates of the droplet boundary, as a function of normalized time. Both pressures and velocities along the interface are of vital importance for the prediction of damage, and pressures within the drop may also be of considerable interest in that they become strongly negative at times during the impact, thus giving rise to the possibility of cavitation during impact (16), which may then add to the damage.

b. Specific results

19. Table 1 lists the most important numerical results, i.e., maximum pressures and radial velocities along the target surface for all the cases studied. The pressures are presented as multiples of both the "simple water-hammer pressure" and the "corrected water-hammer pressure". For the former case, the water-hammer pressure is calculated using the density and sonic velocity for the undisturbed fluid; for the latter, the sonic velocity is corrected according to Eq. (10). The effect of the correction is substantial even at the lower Mach number (about 1.4 for M = 0.2), and much more so for the higher (about 2.0 at M = 0.5). Table I shows that the target surface pressure is nearly independent of Mach number if normalized to the corrected water-hammer pressure (hence, the results in this form can be considered valid over a much larger range of Mach number), and is in all cases substantially less than unity. This fact is ascribed to the additional degrees of freedom for the flow in these two-dimensional problems as compared to the impacting slab one-dimensional case, where the "corrected" water-hammer pressure would indeed be obtained.

20. The target surface pressure exceeds the "simple" (conventional) water-hammer pressure at the lower Mach number only for the cylindrical shape (which is the most unrealistic of those studied due to its sharp corners), and is substantially less in the other cases. However, for 0.5 Mach it exceeds the simple water hammer pressure in all cases (but only by 7% for the spherical drop).

21. Fig. 4, 5, and 6 show the interface pressures at various times during the impact in more detail than do the pressure profiles of Fig. 1, 2, and 3.

22. As is well known (17, e.g.), the radial velocity during impact is usually several times the impact velocity. This result, previously based

*Compressible-Cell-and-Marker method.

primarily upon photographic evidence, is confirmed by the present calculations. Table 1 shows that its maxima range between 2 and 3 times impact velocity (depending upon droplet shape) for the lower Mach number, and between 1.6 and 2.3 for the higher Mach number. The effect of this extremely high liquid velocity upon the target surface through shear and also direct impact upon surface asperities may be very instrumental in the damage process in some cases.

23. A final result of the numerical studies of considerable importance is the discovery of regions of strongly negative pressure within the impacting drops due both to the reflection of pressure waves as tensile waves from the droplet free surfaces, and to the inertia of the outwardly accelerating radial flow along the surface. The pressure profiles of Fig. 7 are illustrative of this situation, which is discussed in more detail elsewhere (6, 7, 16). These results confirm recent photographic evidence showing vapor cavities within impacting drops by Brunton and Camus (18), included here for convenience as Fig. 8. Cavitation within the impacting drop could of course contribute to damage and could help explain observed rapid erosion in pure impact tests at relatively low impact velocity (rapid erosion of stainless steels at 100 m/s is common - (19, e.g.).

B. Additional University of Michigan Turbine Droplet Research

24. Additional portions of our research effort upon the turbine droplet erosion problem include both a newly commenced study of droplet formation in wet steam flow, and actual impact erosion tests. These efforts are described very briefly below.

1. Wet-Steam Tunnel Facility

25. The construction of a low-pressure, wet-steam tunnel is underway in our laboratory at the time of this writing. It is designed to model velocity, moisture, and pressure conditions pertinent to the low-pressure stages of large steam turbines. Moisture film build-up upon submerged surfaces and the subsequent formation and break-off of liquid droplets will be studied photographically. No results are as yet available.

2. Liquid Impact Experiments

26. We have developed and extensively utilized an automated water-gun device (patterned after that of Kenyon (20) producing up to 30 elongated liquid slugs per minute at velocities up to 600 m/s. Liquid slug diameter is about 1 mm (although different diameters can be easily obtained), and their length is the order of 50 dia. The striking edge is approximately hemispherical. As is generally agreed (20, e.g.) and confirmed by our numerical studies already discussed in this paper, generally damagingly high surface pressures and velocities occur only during the very initial portion of impact (fraction of 1 μs), so that only the nose of the liquid slug is important. Thus, while spherical droplets would be preferable for damage studies, the elongated slugs are adequate for the purpose. The shape of slug produced by the gun device is very similar to that obtained by Bowden and Brunton (21), using their single-shot momentum exchange device (also used in our laboratory for more exacting studies of single-drop impact). However, the automated device is far more suitable for experiments involving material resistance to repeated impact. Results of some of this work will be published in the near future. Fig. 9 shows a typical liquid slug from the automated device.

CONCLUDING REMARKS

27. Work from our laboratory related to the turbine droplet impingement problem has been described, while the development of a low-pressure wet-steam tunnel for the study of droplet formation and also experiments upon material resistance to droplet impingement utilizing an automated water gun device are included. The program concerns primarily numerical studies of the actual impingement upon a surface of liquid droplets of various shapes. We believe these to be the first relatively comprehensive numerical studies of this phenomenon. They have produced several relatively important and basic results:

28.1. The maximum pressures generated upon the target surface at least over an appreciable portion of a microsecond, are in general considerably less than the water-hammer pressure, if this is corrected for the increase of shock wave velocity in the compressed liquid. While this pressure would be obtained exactly for a "slab" collision*, the additional degrees of freedom inherent in actual droplet shapes are responsible for the reduced pressure. Of course, the pressures will be further reduced if target surface elasticity (or plasticity) is considered. For impact velocities of the order of 300 m/s, the pressures are also less than the conventional water hammer pressure (shock-wave velocity assumed that of ambient liquid), though they are greater than this value for impact velocities of the order of 750 m/s. The increase over conventional water hammer pressure increases with impact velocity.

29. These results are roughly confirmed by the only applicable experimental measurements of which we are aware, those reported by Brunton (22) and summarized by Hays (23) in 1961. He measured the maximum impact pressure for a jet of 720 m/s velocity (about equivalent to our Mach 0.5 condition), and found that it was 0.875 x "simple water hammer pressure". Since the shape of the droplet is perhaps most similar to our composite shape, his pressure value is less than that which we predict by 1.30/0.875 = 1.50 (see Table 1). The discrepancy may be partly due to inadequate response rate of his transducer.

30. His measurements confirm our estimates of the duration of the high pressure portion of the impact, which he states to be "less than 3 μs, for a drop of about 3 mm. diameter. Duration is of course approximately proportional to diameter.

31.2. If normalized to "corrected "water hammer" pressure" the maximum target surface pressures are nearly independent of impact velocity.

*i.e., the classical one-dimensional case.

32. 3. Radial velocities arising from impact are the order of 2-3 times impact velocity. The multiplying factor decreases with impact velocity over the range studied.

33. 4. Strongly negative pressures arise within the droplet during impact which may give rise to cavitation as already observed photographically (17). Thus the potential for damage may be increased by this phenomenon.

34, 5. Damaging pressure occur only during the initial fraction of a microsecond during a collision for a drop of 2mm dia. The pressure duration is less for smaller drops.

ACKNOWLEDGEMENTS

Financial support for this work was provided primarily under National Science Foundation Grant GK 730.*

REFERENCES

1. HAMMITT, F. G. "Collapsing Bubble Damage to Solids," ASME Cavitation State of Art Symposium, June 1969, pp. 87-102.

2. GARCIA, R., and HAMMITT, F. G., "Cavitation Damage and Correlations with Material and Fluid Properties", Trans. ASME, J. Basic Engr., Vol. 89, Dec. 1967, pp. 755-763.

3. HAMMITT, F. G., "Damage to Solids Caused by Cavitation," Phil. Trans. Roy. Soc. A. No. 1110, 260, 245-255, 1966.

4. HAMMITT, F. G., etal., "Laboratory Scale Devices for Rain Erosion Simulation", 2nd Meersburg Conference on Rain Erosion and Associated Phenomena, August 22-25, 1967, Meersburg, Federal German Republic.

5. HAMMITT, F. G., "Impact and Cavitation Erosion and Material Properties," Proc. 3rd International Rain Erosion Congress, Farnborough, England, Aug. 1970.

6. HUANG, Y. C., "Numerical Studies of Unsteady, Two-Dimensional Liquid Impact Phenomena," PhD Thesis, The University of Michigan 1971; also available as ORA Report No. UMICH 033710-8-T, 1971.

7. HUANG, Y. C., HAMMITT, F. G., YANG W-J, "Hydrodynamic Phenomena During High Speed Collision between Liquid Droplet and Rigid Plane," May 1972, submitted to ASME; also available ORA Report UMICH 03371-16-T.

8. HUANG, Y. C., HAMMITT, F. G., "Liquid Impact on Elastic Solid Boundary," Prog. 11th Symp. on Electromagnetic Windows, Geo. Inst. Tech., July, 1972.

9. TAIT, P. G., "Report on Some of the Physical Properties of Fresh Water and Sea Water," Report on Scientific Results of Voy, H. M. S., and Challenger, Phys. Chem., 2, 1-71 (1888).

10. HUANG, Y. C., HAMMITT, F. G., MITCHELL, T. M., "A Note on Shock Wave Velocity in High-Speed Liquid-Solid Impact," to be published J. Appel. Phys.; also ORA Rept. UMICH 033710-11-T, Sept., 1971.

11. HEYMANN, F. J., "On the Shock Wave Velocity and Impact Pressure in High-Speed Liquid-Solid Impact," Trans. ASME, J. of Basic Engr., 90, p. 400, July 1968.

12. HUANG, Y. C., HAMMITT, F. G., and YANG, W-J, "Mathematical Modelling of Normal Impact between a Finite Cylindrical Liquid Jet and Non- Slip Flat Ridgid Surface," Submitted for publication to 1st Internation Symposium on Jet Cutting Technology, BHRA; also available as ORA Report No. UMICH - 03371-13-T, Univ. of Mich.

13. AMSDEN, A. A., "The Particle-in-Cell Method for the Calculation of the Dynamics of Compressed Fluids," Los Alamos Scientific Lab., Report No. LA-3466 (1966).

14. WELCH, J. E., HARLOW, F. W., SHANNON, J. P., and DALY, B. J., "The MAC Methods," Los Alamos Scientific Lab., Report No. LA-3425 (1960).

15. LAX, P. and WENDOROFF, B., "System of Conservation Laws," Communication on Pure and Applied Mathematics, XIII, pp. 217-239 (1960).

16. HUANG, Y. C., HAMMITT, F. G., "Cavitation within an Impinging Liquid Droplet," 1972 Polyphase Flow Forum, ASME; also available as ORA UMICH 03371-15-I, 1972.

17. FYALL, A. A., "Single Impact Studies of Rain Erosion," Shell Aviation News, 374, (1969).

18. BRIGGS, L. J., "Limiting Negative Pressure of Water," J. of Applied Physics, 21, July 1950, pp. 721-722.

19. CANAVELIS, R., "Comparison of the Resistance of Different Material with a Jet Impact Test Rig," HC/061-230-9, Electricite de France, Chatou, France, Nov., 1967.

20. KENYON, H. F., personal communications to F. G. Hammitt, 1967-1970.

21. BOWDEN, F. P., and Bruton, J. H., "The Deformation of Solids by Liquid Impact at Supersonic Speeds," Proc. of the Royal Society, A, 263, pp. 433-450, (1969).

22 BRUNTON, J. H., "Deformation of Solids by Impact of Liquids at High Speed," ASTM STP 307, 1961, pp. 83-98.

23. HAYS, L. G., "Turbine Erosion Research in Great Britain," NASA Tech. Memo No. 33-271, Jet Prop. Lab., Pasadena, Cal., March 1966.

*The steam tunnel has been designed by Prof. J. Krzyzanowski of IMP PAN, Gdansk, Poland, who was resident in our laboratory during the spring of 1972.

Symbol	Notation
A	Exponent in Tait's equation of state
B	Constant in Tait's equation of state
A_1, A_2, B_1, B_2	Dimensionless coefficients
C	Shock wave velocity
C_o	Sonic velocity
H_1, H_2	Dimensions of Computation Domain in z- and r-direction, respectively
P	Pressure
R_m	Location of marker m in r- coordinate
r	Radial coordinate
t	Time
U	Marker velocity component in z-direction
u	Velocity component in z-direction
V	Marker velocity component in r- direction
v	Velocity component in r- direction
v_t	Velocity component in tangential direction
z	Vertical coordinate
ρ	Density
	Subscripts
m	Marker index
n	Normal direction
o	Initial value
t	Tangential direction

TABLE I

Summary of Principal Numerical Results

	M = 0.2 (V_o = 300 m/s)			M = 0.5 (V_o = 750 m/s)		
	$\frac{Pmax}{\rho_o C_o V_o}$	$\frac{Pmax}{\rho_o CV}$	$\frac{Vmax}{V_o}$	$\frac{Pmax}{\rho_o C_o V_o}$	$\frac{Pmax}{\rho_o CV_o}$	$\frac{Vmax}{V_o}$
Free Slip Wall Boundary						
	1.17	0.84	2.00	1.61	0.82	1.65
	0.69	0.495	2.65	1.07	0.52	2.15
	0.90	0.65	2.80	1.30	0.66	2.25
Non-Slip Wall Boundary						
	1.20	0.87	2.10	1.675	0.85	1.70
	0.80	0.59	2.85	1.229	0.625	2.30
$\rho_o C_o V_o = \rho_o V_o^2 / M =$		4450 bars			11,100 bars	

3428

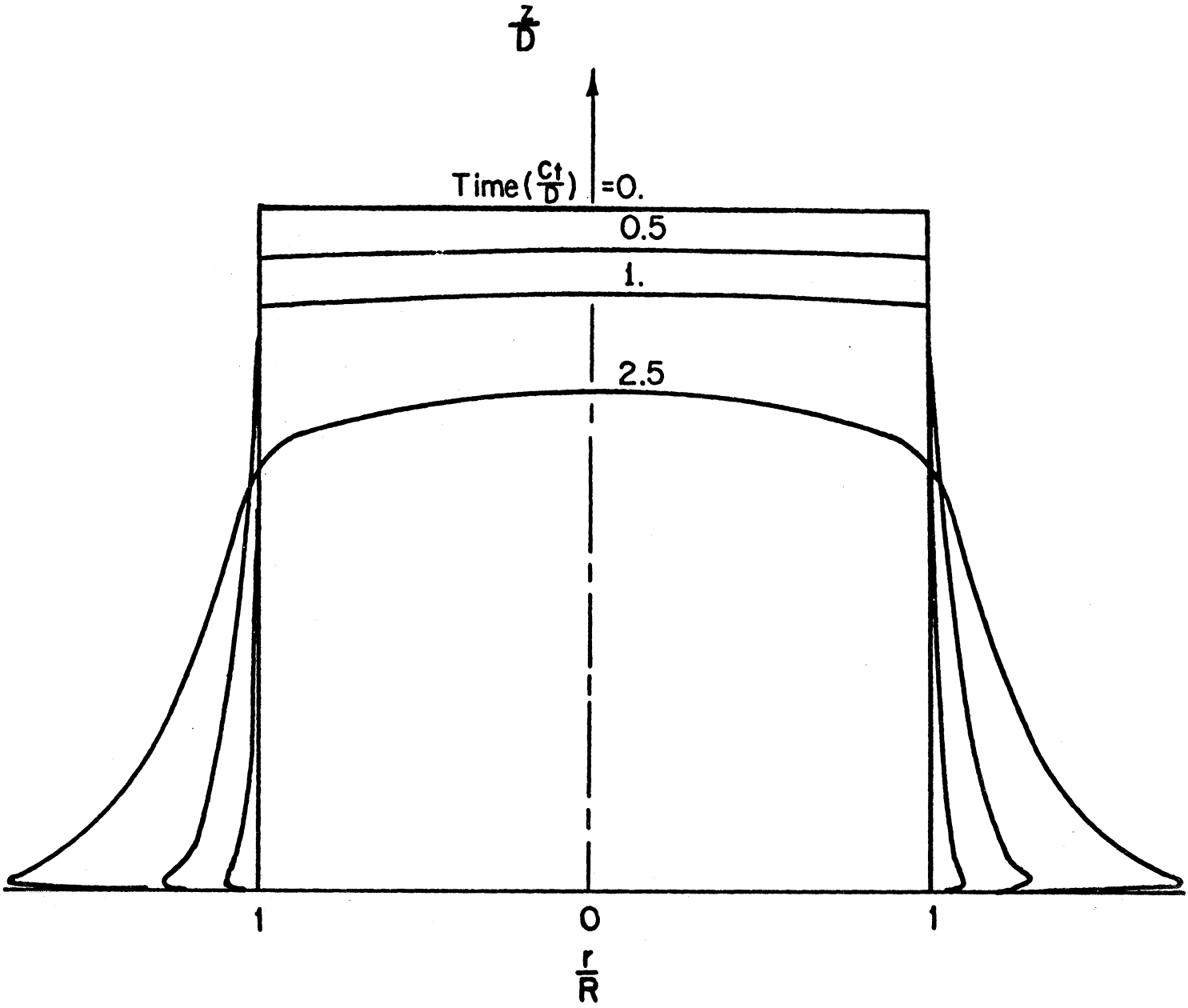

($t^o = \frac{Ct}{D} \cong 1\ \mu s$ for 2mm drop)

Fig. 1 Shape-Time History of an Initially Cylindrical Droplet with L/D = 1, at Mach Number = 0.2, for Free-Slip Boundary Condition.

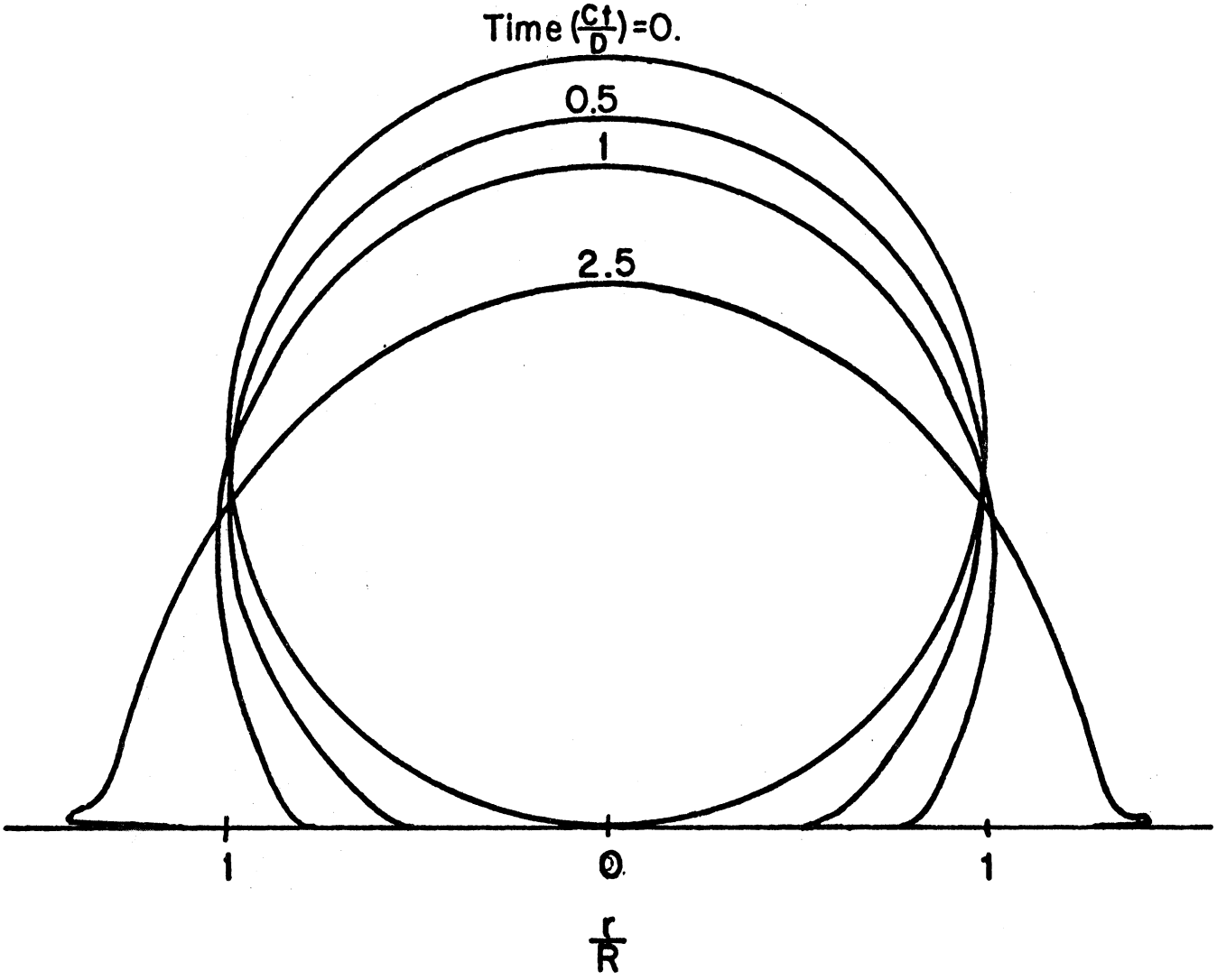

$(t^o = \frac{Ct}{D} \cong 1\ \mu s$ for 2mm drop)

Fig. 2 Shape-Time History of an Initially Spherical Droplet at Mach Number = 0.2, for Free-Slip Boundary Condition.

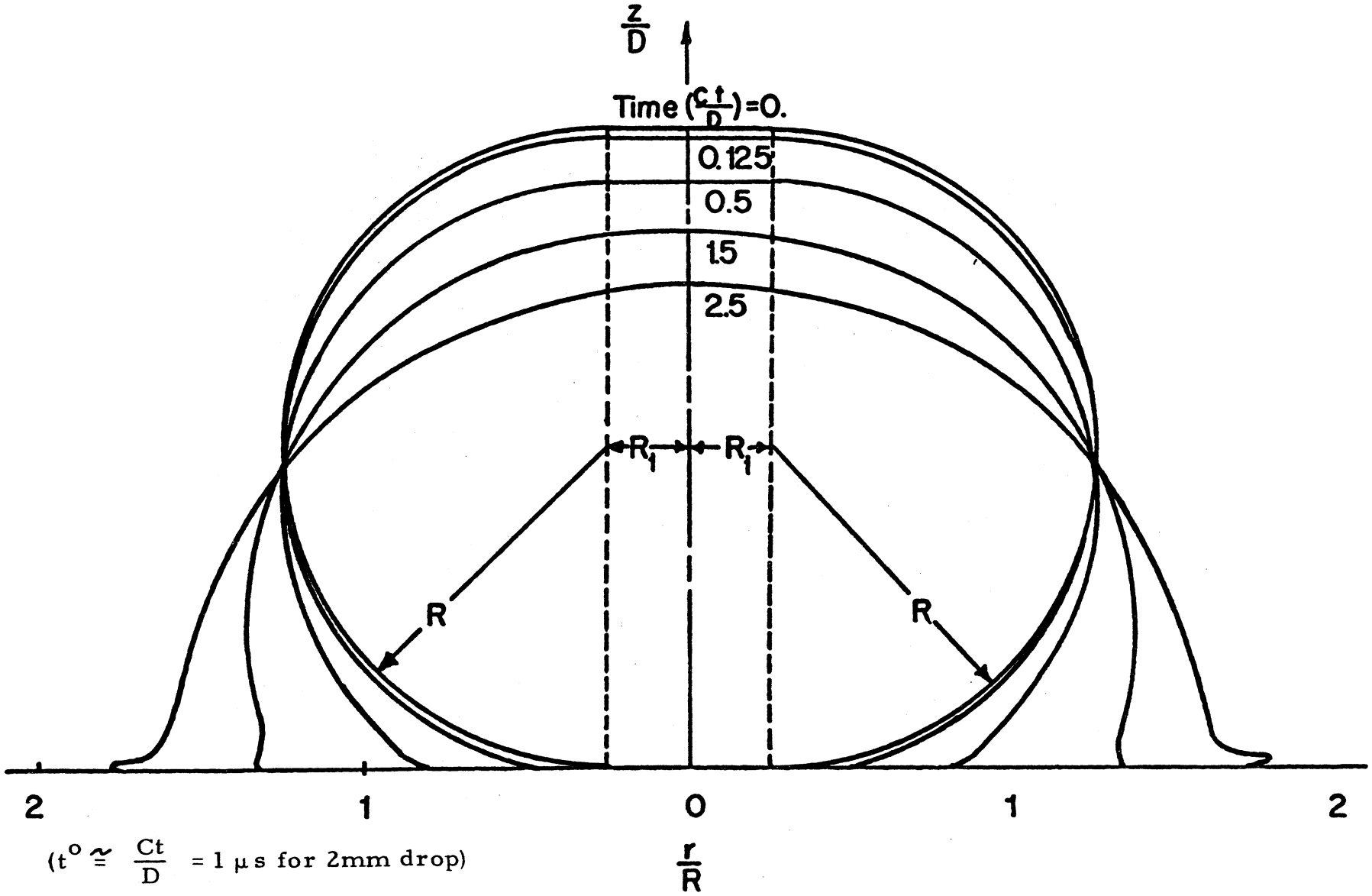

Fig. 3 Shape-Time History of an Initially Cylindrical-Spherical Composite Droplet with $R_1/R = 0.25$ and $L/D = 1$, at Mach Number = 0.2, for Free-Slip Boundary Condition.

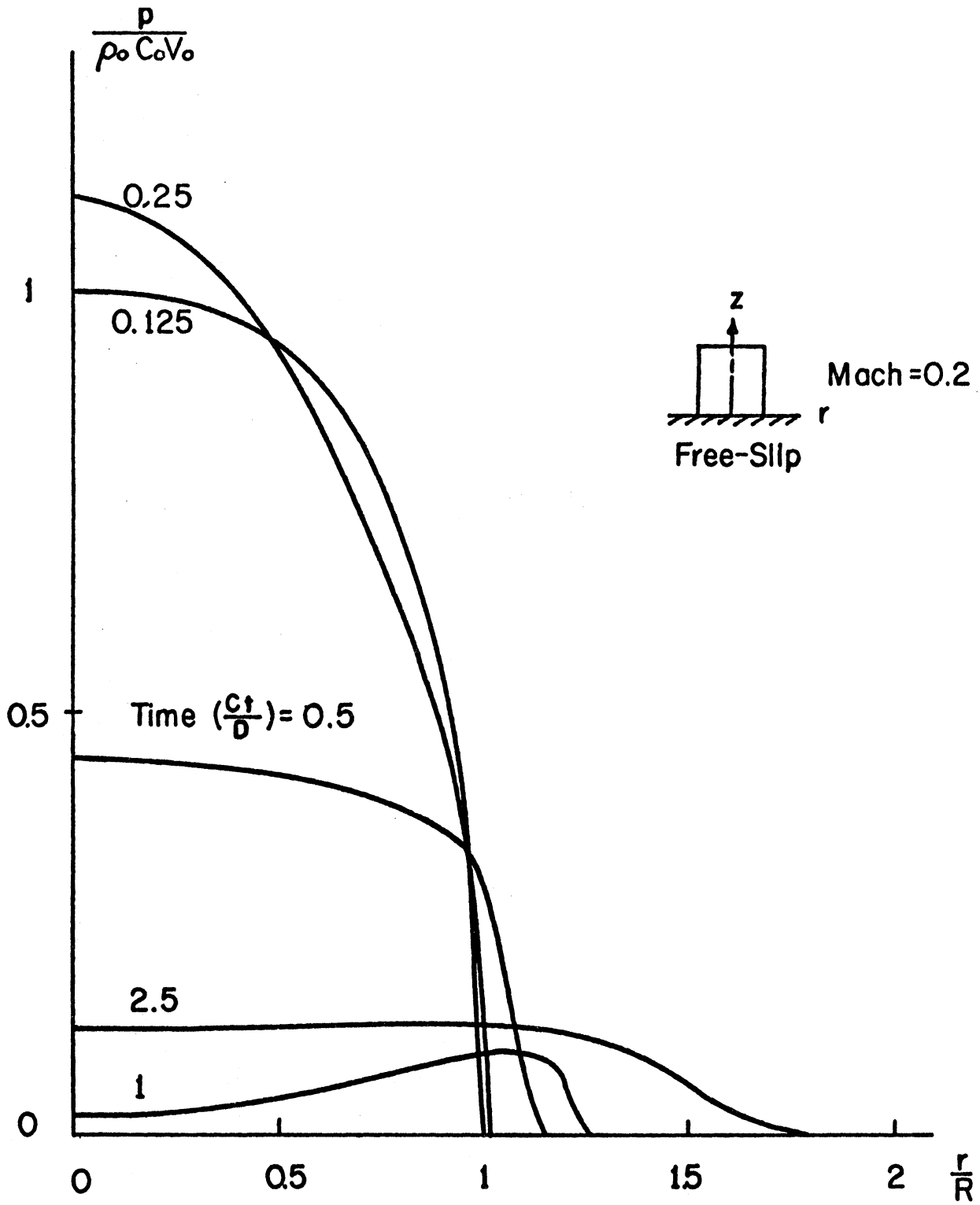

($t^o = \frac{Ct}{D} \simeq 1\ \mu s$ for 2mm drop)

Fig. 4. Pressure-Time History at Liquid-Solid Interface (z = 0) of an Initially Cylindrical Droplet with L/D = 1, for Impact Mach Number of 0.2 and for Free-Slip Boundary Condition.

3395

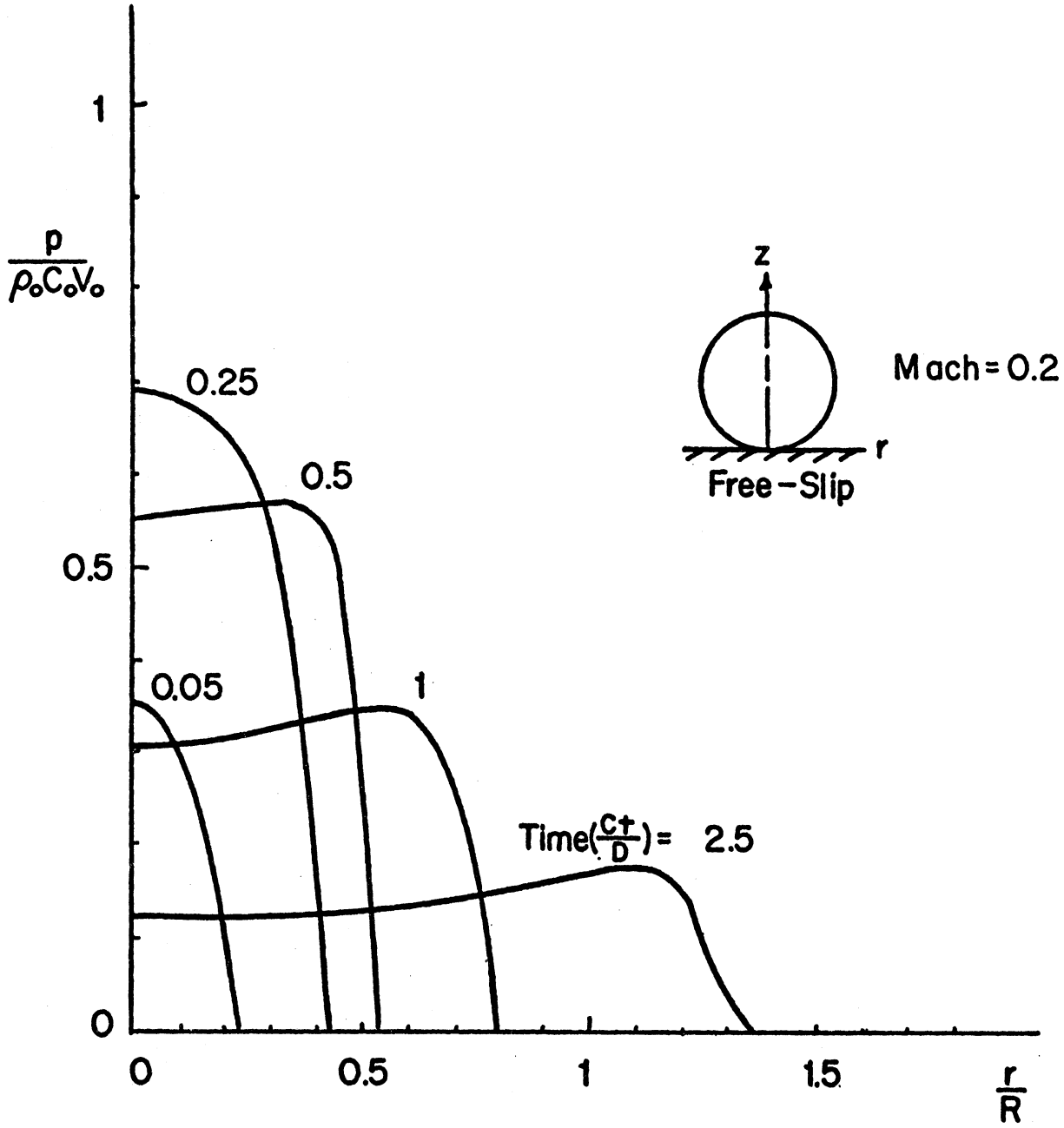

Fig. 5 Pressure-Time History at Liquid-Solid Interface (z = 0) of an Initially Spherical Droplet for Impact Mach Number of 0.2 and for Free-Slip Boundary Condition.

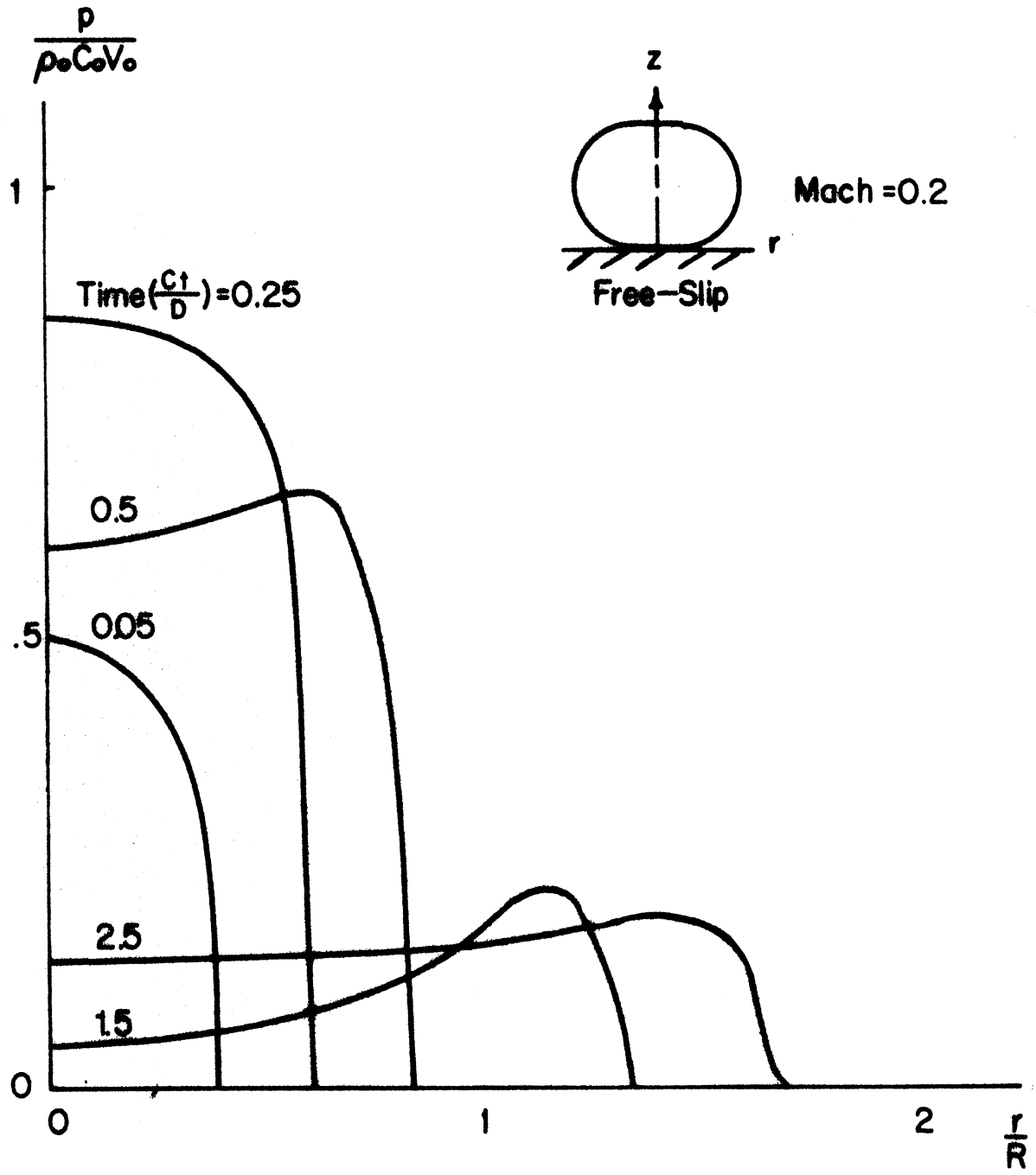

Fig. 6. Pressure-Time History at Liquid-Solid Interface (z = 0) of an Initially Cylindrical-Spherical Composite Droplet with R_1/R = 0.25 and L/D = 1, for Impact Mach Number of 0.2 and for Free-Slip Boundary Condition.

3402

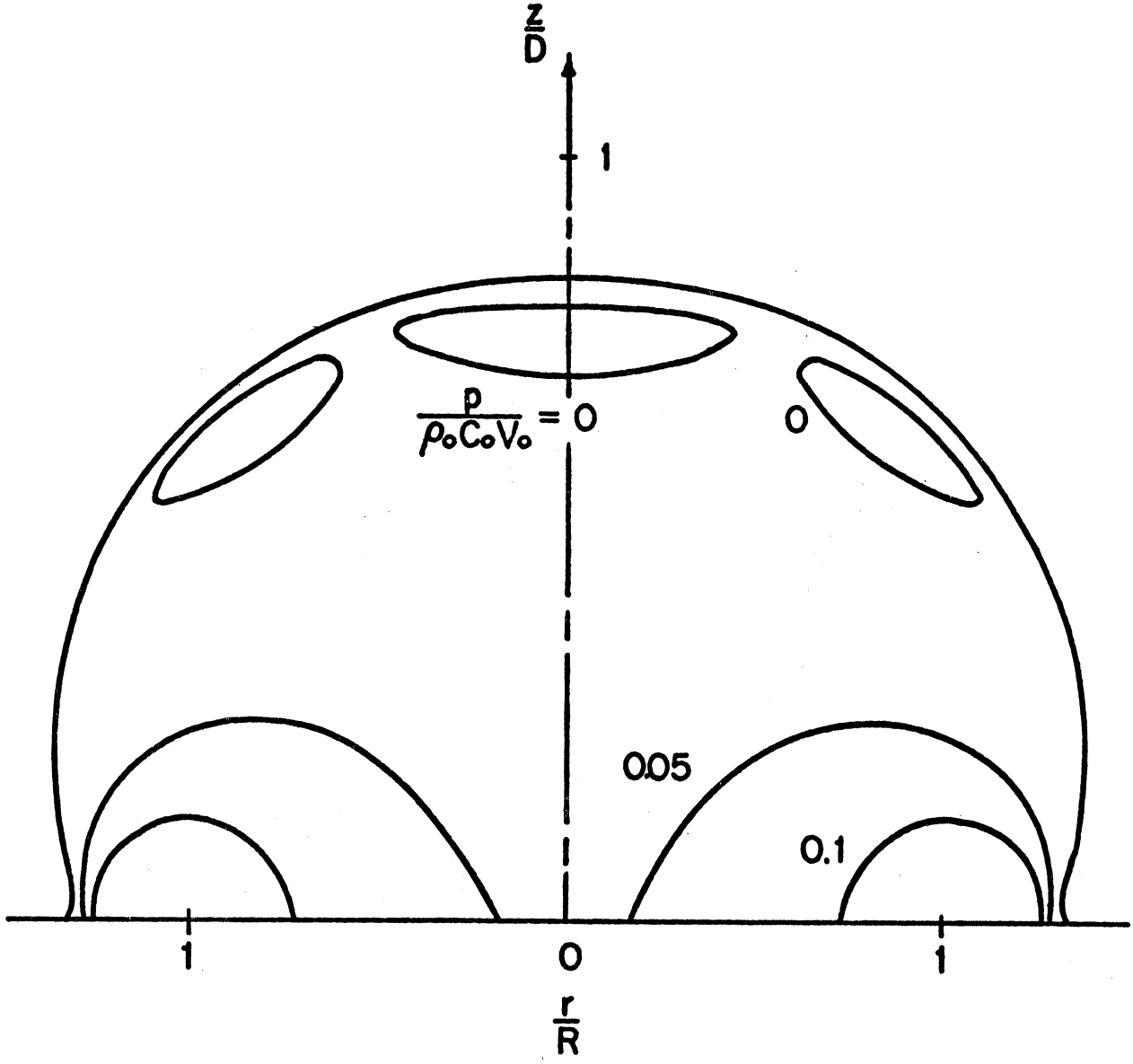

$(t^o = \frac{Ct}{D} \simeq 1\ \mu s$ for 2mm drop)

Fig. 7 Isobar Distribution in an Initially Cylindrical-Spherical Composite Droplet with $R_1/R = 0.25$ and $L/D = 1$, at Time $(Ct/D) = 1.5$ for Impact Mach Number of 0.2 and for Free-Slip Boundary Condition.

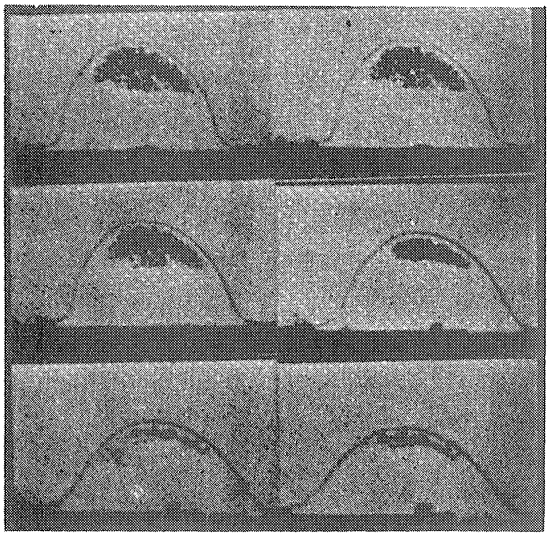

Fig. 8 Photographs of the Cavitation for a Water Droplet Following an Impact on a Solid Plane (Brunton and Camus[38])